



Investigation of structural, morphological and nonlinear optical properties of ZnO thin films using reflective Z-scan technique

Getu Endale^{1,2} · Poonam Loura¹ · Devendra Mohan¹

Received: 22 March 2023 / Accepted: 14 September 2023 / Published online: 7 October 2023

© The Author(s), under exclusive licence to Springer Science+Business Media, LLC, part of Springer Nature 2023

Abstract

Zinc Oxide is an n-type direct bandgap (3.2 eV) material having large exciton binding energy of (60 meV) and strong optical nonlinearity. Zinc Oxide thin films plays crucial role in revolutionizing performance of optical and electrical devices. In this study, laser-induced third-order optical nonlinearity in Zinc oxide thin film samples are investigated. This method is used to investigate the nonlinear refraction using the high-intensity source. Zinc oxide has been deposited on p-type silicon substrate using sol–gel techniques with various substrate temperature of room temperature (RT), 300 °C, and 500 °C. The samples have been characterized by X-ray diffraction studies. And the deposited zinc oxide film shows hexagonal wurtzite structure and the lattice parameters change with substrate temperature. Surface morphology of Zinc oxide thin film samples are analysed using FE-SEM and branching like urchin morphology is observed and the size of rods and crystallites of thin films increases, when temperature is varied. A pulsed laser beam having a wavelength of 532 nm has been used as the excitation source. Reflective Z-scan (RZ-scan) technique of open aperture was performed, since zinc oxide thin film samples are opaque. Normalized reflectance is fitted to experimental data to calculate nonlinear reflective index, n_2 of the sample and the values of n_2 estimated for room temperature (RT), 300 °C, and 500 °C are $1.5 \times 10^{-9} \text{ cm}^2/\text{W}$, $2.9 \times 10^{-9} \text{ cm}^2/\text{W}$ and $25.3 \times 10^{-9} \text{ cm}^2/\text{W}$.

Keywords RZ-scan · Zinc oxide · Sol–gel technique · XRD · FE-SEM · Thin film

✉ Getu Endale
getuendale1@gmail.com

Poonam Loura
poonamloura93@gmail.com

Devendra Mohan
vand66@yahoo.com

¹ Physics Department, Guru Jambheshwar University of Science and Technology, Hissar 125001, India

² Physics Department, Wolkite University, Wolkite, Ethiopia

1 Introduction

Now a days, semiconducting thin films have attracted many researchers because of they are used in the investigation of the fundamental studies of size and dimensions in their physical characteristics. Linear, and nonlinear Non-linear optical characteristics of materials have significant impact in developing new engineering technologies such as quantum computing, (Zidan 2020), quantum memories (Zidan et al. 2021), and quantum technologies (Zidan et al. 2023, 2022; Liu et al. 2022). Also, Non-linear optical characteristics of Zinc Oxide thin films are studied due to its high applications in optoelectronic devices development (Zidan et al. 2021; Zidan et al. 2023). ZnO is a wurtzite II–VI n-type direct band gap (~ 3.3 eV at room temperature) materials having large exciton binding energy of (60 meV) and has been broadly studied for electronic applications (Zidan 2020, 2021). Non-linear optical characteristics of Zinc Oxide thin films are studied due to its high applications in optoelectronic devices development. ZnO is a wurtzite II–VI n-type direct band gap (~ 3.3 eV at room temperature) materials having large exciton binding energy of (60 meV) and has been broadly studied for electronic applications (Bacaksiz et al. 2008; Chen et al. 2003). Zinc Oxide thin films have been studied by many researchers due to its many advantages over other oxide thin films, like non-toxicity, good optical and electrical behaviour, high binding energy, good conductivity, stability in hydrogen plasma and available in low price (Chaari and Matoussi 2012; Li et al. 2004; Mosca et al. 2011; Laurenti and Cauda 2018).

The optical nonlinearity of ZnO based thin films and its derivatives are widely studied. Litty Irimpan et al. (2008) investigated the NLO properties of assembled films formed from ZnO colloidal spheres using modified polyol precipitation method followed by drop casting technique. The size dependence and intensity dependence of the samples was investigated using a Q-switched Nd: YAG laser (532 nm, 7 ns, 10 Hz) and the wavelength dependence of the samples were studied using a tunable laser (5 ns, 10 Hz). Z-Scan study revealed switching from reverse saturable absorption to saturable absorption as the material changes from colloid to self-assembled film at an intensity of 220 MW/cm². These different nonlinear characteristics can be mainly attributed to ZnO defect states and electronic effects when the colloidal solution is transformed into self-assembled monolayers. Self-defocusing effect leading to negative nonlinear refractive index in ZnO thin films grown on glass-substrate by sol–gel method is reported by Kepceo et al. (2019). Single beam Z-scan with 532 nm laser wavelength led to determination of the nonlinear absorptive behaviour and the sign of nonlinear index of refraction. The films displayed large nonlinearity and a numerical fit to the experimentally obtained curves for the single layer ZnO film provided the values of two-photon absorption coefficient (β) as 3.7×10^{-5} m/W, imaginary part of third order susceptibility (χ^3) as 3.35×10^{-14} m²V⁻² and the nonlinear refractive index (n_2) as 2.5×10^{-4} esu.

A variety of deposition techniques have been developed for the fabrication of zinc Oxide thin films. These techniques are chemical vapour deposition, pulsed laser deposition (PLD), RF-sputtering and sol–gel (Growbaska et al. 2005; Morosanu 1990). From all of these techniques, sol–gel method is good due to its sophisticated working phenomena and rapid deposition process, which takes more time when compared to other deposition techniques (Constantinescu et al. 2015; Boyd 2013). Sol–gel method build high quality films of all chemical compositions, which is fast, simple, cost-effective, scalable and versatile (Zhu et al. 2015; Zhang et al. 2015; Vanalakar et al. 2015; Li et al. 2015; Tite et al. 2014; Bäuerle 2013; Oruç et al. 2012).

The purpose of this work is to produce a c-axis oriented opaque thin film of ZnO on a silicon wafer using sol-gel method at various substrate temperatures: room temperature (RT), 300 °C and 500 °C. Because our samples are opaque and have no transparency, we experimentally analyse optical non-linear characteristics of zinc oxide thin film samples using RZ-Scan. The method analyses amplitude & phase properties of reflected beam as it passed through the opaque samples. When a high-powered laser light having wavelength of 532 nm, with a pulse width of 5 ns collides with the surface of a sample, it changes its optical characteristics. These changes are caused by nonlinear optical phenomena and other energy transformation mechanisms and studied using RZ-Scan technique. It investigates spatial shape of laser beam after reflection from a sample tilted at an angle of 30° positioned at the focal plane of the convex lens. The technique is useful because of it puts less stress on ZnO thin sample, requiring only a single shot of the laser pulse to determine nonlinear refractive indices.

The rest of this paper is organized as follows: Sect. 2 describes experimental investigations of measuring nonlinearities of ZnO thin film sample using Z-scan techniques. Section 3 presents result and discussion of nonlinear optical properties and characterization techniques. Finally, Sect. 4 reflects conclusion parts.

2 Experimental technique

Crystalline opaque zinc oxide thin film samples of S1, S2 and S3 are deposited on silicon substrate. The samples S1, S2 and S3 are deposited at various temperatures of (RT), 300 °C and 500 °C respectively, by using sol-gel technique. For deposition ZnO material is used as the host material and by using a Desktop X-ray Diffractometer (Rigaku, MiniFlex-II), the crystallographic structural properties of zinc oxide thin film samples were investigated. CuK_{α} (1.541Å) radiation was used to obtain the XRD patterns in the wide-angle ranges varying from 10° to 80°.

To analyse nonlinear optical characteristics of zinc oxide samples, reflective z-scan techniques were made, as its experimental set-up is illustrated in Fig. 1 below. As an optical energy source, a continuous wave (cw) diode laser (TCLDM9 Thorlabs) with a Gaussian beam profile of wavelength 532 nm with controlled power of 120 mW was focused by a lens of 150 mm focal length (A). A zinc oxide thin film sample (B) was mounted to the translation table (K) & moved along the z-axis. When the sample is moved along optical

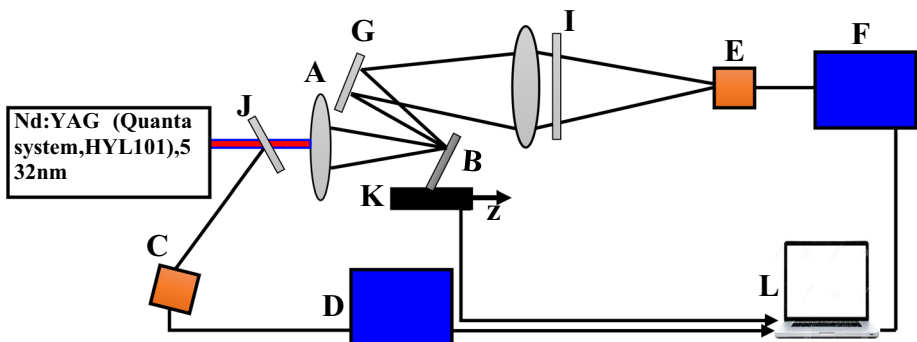


Fig. 1 Schematic diagram of Reflective z-scan for nonlinear optical measurement

axis, it passes through the focal region of lens (A), at an angle of incidence of laser radiation on the surface of sample 30° . A step motor was used to move the sample on the micro-metre table (K). Some of radiation reflected from the beam splitter (J) was recorded by silicon detector photo-diode (DET-110, Thorlabs) (C), placed before the focusing system to manage the energy of laser pulses. Radiation reflected from the surface of sample was directed to the deflecting mirror (G) and synchronized with movable table (K). Then, all reflected radiations are gathered by lens (H) and registered by photo-diode (E), that is prevented from optical damage by neutral filters (I). The signals received by photodiodes (C) & (E) were sent to the inputs of stroboscopic voltage transducers (D) and (F). Digital signals from both stroboscopic voltage transducers received by a controller, which was linked to a personal computer (L).

To minimize the effects of fluctuations of the laser radiation intensity, the signal intensity reflected by zinc oxide thin film sample (I_R) was normalized to signal intensity of the incident laser radiation I_0 . The experimental intensities were expressed as normalized reflectance $R(z) = I_R/I_0$ versus locations of a sample along z-axis.

3 Results and discussions

3.1 X-ray diffraction (XRD) studies

Structural characteristics of zinc oxide thin film samples at various substrate temperatures have been investigated by XRD patterns in the range of angle $10^{\circ} - 80^{\circ}$ using CuK_{α} (1.541\AA) radiation. The deposited films on silicon substrate shows diffraction peaks that indicates the crystalline nature of the sample at all various temperatures of (RT), 300°C and 500°C .

Figure 2 indicates XRD plot for Zinc oxide thin films of samples S1, S2 and S3 for various substrate temperatures of (RT), 300°C and 500°C respectively. Diffraction peaks with 2θ values of 68.4, 33.58, 68.41, 71.83 and 33.29 corresponding to (112), (002), (200), (201) and (002) planes of ZnO are indicated at room temperature (RT), 300°C and 500°C respectively. Zinc oxide thin film samples deposited at substrate temperatures RT & 300°C indicates synthesis of various solid solutions and the film deposited at 500°C shows a strong reflection at $2\theta = 33.29(002)$ which is predominant peak. This indicates the sample shows excellent c-axis alignment perpendicular to substrate and hexagonal wurtzite structure (JCPDS card 00–036–1451) with lattice parameter $a = b = 3.11\text{\AA}$, and $c = 5.38\text{\AA}$. The red shift is due to the heating of substrate which causes coalesce of grain boundaries, which means there is a change in D as indicated in Table 1 below.

Debye–Scherrer’s formula was used to determine grain size (Song et al. 2002):

$$D = \frac{0.95\lambda}{\beta \cos\theta} \quad (1)$$

Here, $\lambda = 1.541\text{\AA}$ for CuK_{α} line & β is Full Width at Half Maximum (FWHM) at 2θ .

The grain size increases from 0.31 at RT and 0.70 at 500°C , which indicates that as substrate temperature increases, grain size of Zinc oxide thin films of samples also increases. This is due to the increase of holding time and heating temperature that will increase the activation energy of growth which will negate previous dislocations that exists on the grain boundaries. At high temperature (500°C), diffraction peak (002) becomes stronger which is in agreement with previous literature (Banerjee et al. 2006a; Kim et al. 2004; Ma et al.

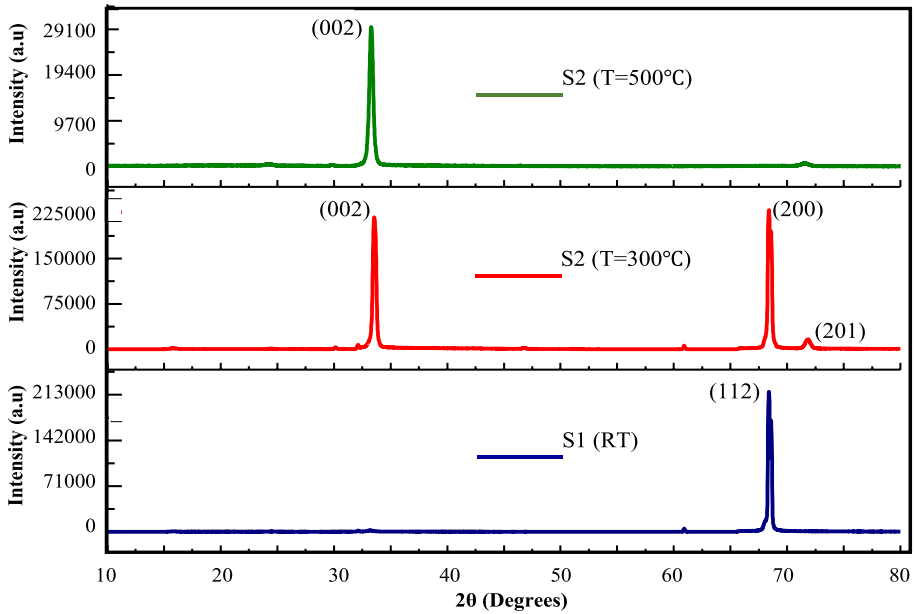


Fig. 2 X-ray diffraction patterns of Zinc oxide thin film samples deposited at temperatures of RT, 300 °C & 500 °C

Table 1 Structural characteristics of zinc oxide thin film samples of various substrate temperatures estimated from X-ray Diffraction

ZnO Thin films	Angle (2θ)	Full width at half maximum (FWHM) (β)	Planes (hkl)	Lattice parameter (d_{hkl}) in (Å)	Grain size (D) in nm
S1 (RT)	68.4	0.249	(112)	2.74	0.31
S2 (300 °C)	33.5	0.358	(002)	2.67	0.38
	68.41	0.249	(200)	2.74	0.42
	71.83	0.584	(201)	3.94	0.51
S3 (500 °C)	33.29	0.399	(002)	2.69	0.70

1996; Fan et al. 2005). The sample at this temperature exhibited a single (002) peak that matched to the c axis alignment perpendicular to substrate Dikovska et al. 2005). Table 1 represents structural characteristics of zinc oxide thin film samples for various substrate temperatures estimated from X-ray Diffraction.

The strain ϵ in the films were estimated from line broadening using (Yakubu et al. 2015):

$$\epsilon = \frac{\beta \cos\theta}{4} \quad (2)$$

Lattice constants c and a are calculated from the X-ray Diffraction (Schroder 1990) and values of lattice parameters are listed in Table 1.

$$\frac{1}{d_{hkl}} = \sqrt{\frac{4}{3} \left(\frac{h^2 + k^2 + hk}{a^2} \right) + \frac{l^2}{c^2}} \quad (3)$$

3.2 Field emission scanning electron microscope (FE-SEM) studies

Surface morphology of Zinc oxide thin film samples are analysed using FE-SEM. Figure 3 below indicates FE-SEM images of Zinc oxide thin film samples for various substrate temperature. The morphology of the ZnO sample grown at room temperatures RT, 300 °C and 500 °C are shown in Fig. 3. The sample is primarily made up of cluster of ZnO nano-rods. As substrate temperatures increases from 300 to 500 °C, branching like urchin morphology is observed and the size of rods and crystallites of thin films increases.

3.3 Fourier transform infra-red spectroscopy (FTIR) studies

FTIR Spectroscopy is used to study vibrational properties of zinc oxide thin films. Absorption peaks and band positions are depend on morphology, structure and chemical

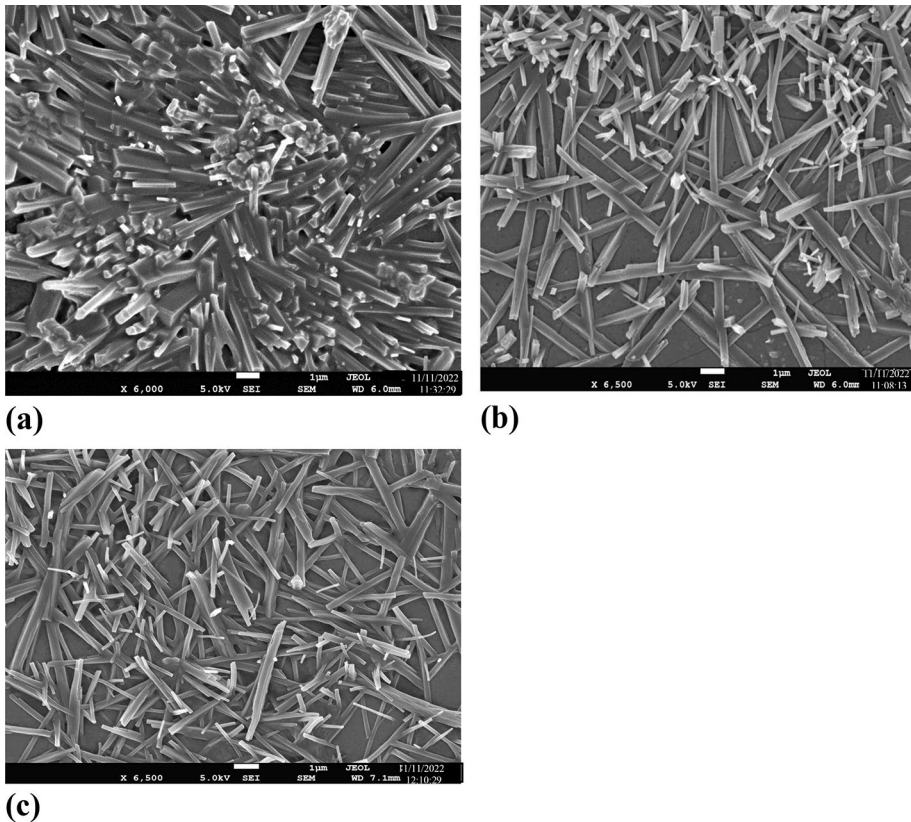


Fig. 3 FE-SEM images of Zinc oxide thin films samples deposited at substrate temperature of RT, 300 °C and 500 °C

compositions of thin films (Yang et al. 2009). Reflection spectrum of zinc oxide thin films on Si substrate are shown in Fig. 4a–c below. Nicolet Magana IR750 FTIR spectrometer was used to study Structural and functional group vibrations of zinc oxide thin films in the wave number range 400cm^{-1} to 1500cm^{-1} . The band observed in the range of $430 - 632\text{cm}^{-1}$ corresponding to the vibrational stretching mode is surrounded with tetragonal ZnO atoms as reported by several studies (Sagadevan et al. 2019). The broad peak in the range of $861 - 968\text{cm}^{-1}$ is attributed to water molecules found in zinc oxide thin film. Weak peak at 1439.61cm^{-1} is attributed to symmetric C = O bond vibration and substrate temperature variations (Rajalekshmi and Raj 2021).

3.4 UV–visible analysis optical absorption and optical band gap

Optical characterization used to follow the evolution and allow studying how the heat treatment affects the transmittance of the thin films. Transmittance (T), reflectance (R) and absorbance (A) characterize the interaction of incident radiation with a particular coating material and are used to study Optical characterization.

Absorbance of zinc oxide thin film calculated by Willey (1936):

$$A + T + R = 1 \quad (4)$$

Optical absorbance spectra of zinc oxide thin film samples deposited at various temperature of (a) RT, (b) 300°C and (c) 500°C in the wavelength range of $100\text{nm} - 1200\text{nm}$ are analysed by using UV–Visible spectrometer. Absorbance spectrum of zinc oxide thin

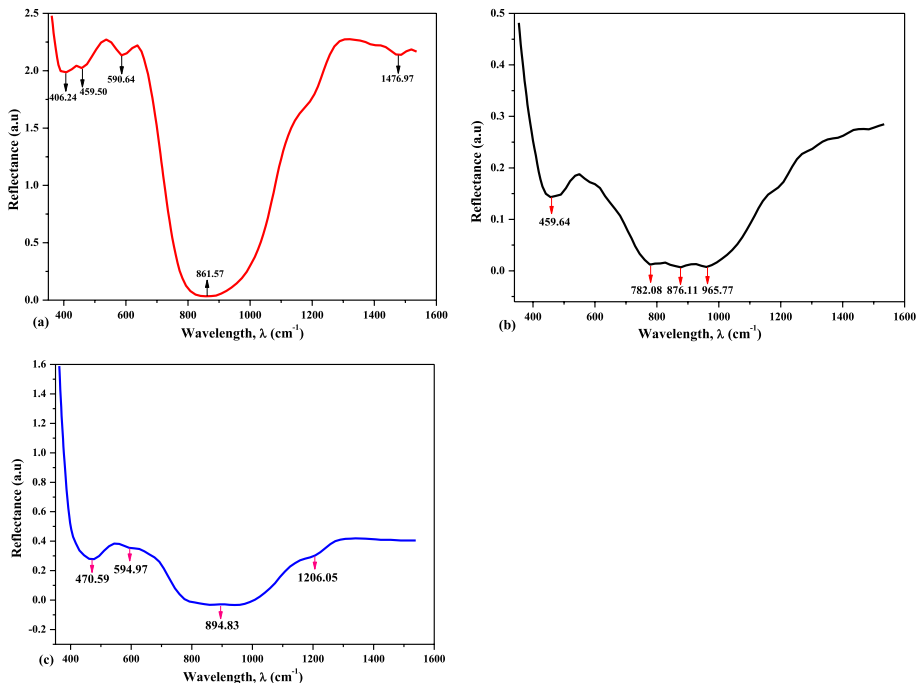


Fig. 4 FTIR spectrum of Zinc Oxide thin film deposited at **a** RT, **b** 300°C and **c** 500°C

film samples are reported in Fig. 5 below. The figure indicates, absorbance of zinc oxide thin film decreases with the increasing of substrate temperature.

The presence of two absorption peaks at around 316 nm and 360 nm for all the film are identified. The absorption peak around 316 nm refers to the excitonic absorption. This excitonic absorption peak lies significantly below the 360 nm i.e., band gap of ZnO, is associated with the quality of nanoparticle distribution (Talam et al. 2012). The strong absorption peak around 360 nm is the characteristic of ZnO film. All the film shows high optical absorbance of $\geq 80\%$ in visible region.

The transmittance drops appreciably around 370 nm in UV region and it is the intrinsic band gap of zinc oxide thin film (3.3 eV). Shifts in absorption edge towards lower wavelength regime for the film deposited at various substrate temperature is displayed. It is observed for all the film, the transmittance decreases below 400 nm, because of the fundamental absorption edge attributed to the electron, that makes cross over from valance band to conduction band. Changes in optical transmittance of the film is associated to surface roughness and the virtue of crystallinity of ZnO film (Srinivasulu et al. 2017).

Band gap energy, E_g calculated by considering a direct transition between valence & conduction bands by using the following equation:

$$\alpha = \frac{A(h\nu - E_g)^{\frac{1}{2}}}{h\nu} \quad (5)$$

Here, h is Planck's constant, ν is frequency of incident radiation, and A is absorbance.

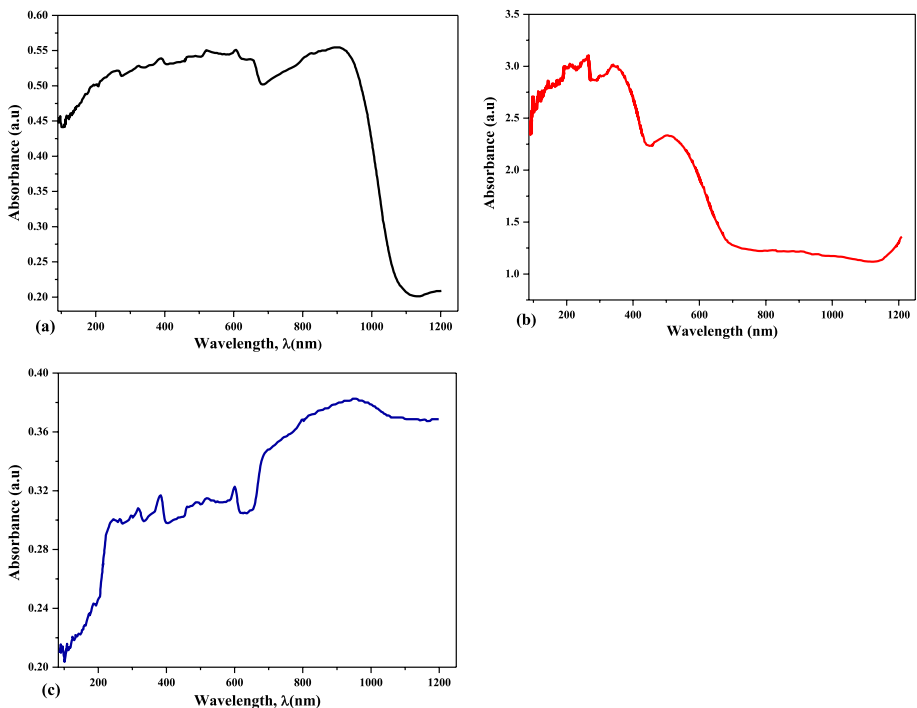


Fig. 5 UV-V Absorbance spectrum of ZnO thin film **a** at room T, **b** at T of 300 °C and **c** at T of 500 °C

Values of energy band gap, E_g is obtained from the graph of $(\alpha hv)^2$ vs. (hv) by extending the straight-line part of $(\alpha hv)^2 = 0$ using Touc's plot techniques as indicated in Fig. 6. E_g of 3.46, 3.41 and 3.14 for zinc oxide thin film samples of S1, S2 and S3 are obtained which shows strong agreement with previously obtained values of energy band gap values of bulk (Suchea et al. 2007).

The linearity noticed from the graph represents the direct transition of band gap of semiconductor. Energy band gap of zinc oxide thin film samples ranged from 3.46 to 3.14 eV. The film deposited at room temperature was 3.14 eV and this trend in band gap may be due to the appearance of band tail from defects and surface roughness (Sadananda Kumar et al. 2013). Decrease in optical band gap as temperature increase is associated with the interatomic distance and caused by the improvement of crystallization in zinc oxide thin film (Komaraiah et al. 2016). The observed energy band gap values agree with earlier reports (Sandeep et al. 2017; Srinatha et al. 2017).

3.5 Investigation of nonlinear optical properties

Nonlinear optical properties of zinc oxide thin films were studied using reflective z-scan techniques (Martinelli et al. 2000). Radiation reflected from the surface of thin film sample is expressed as:

$$I_R(z) = I_0 \left| \left(R_0 G_0^{-1}(z) + R_1(\theta)(n_2 + ik_2)I(z)G_1^{-1}(z_1)(1 - ix) \right)^2 \right| \quad (6)$$

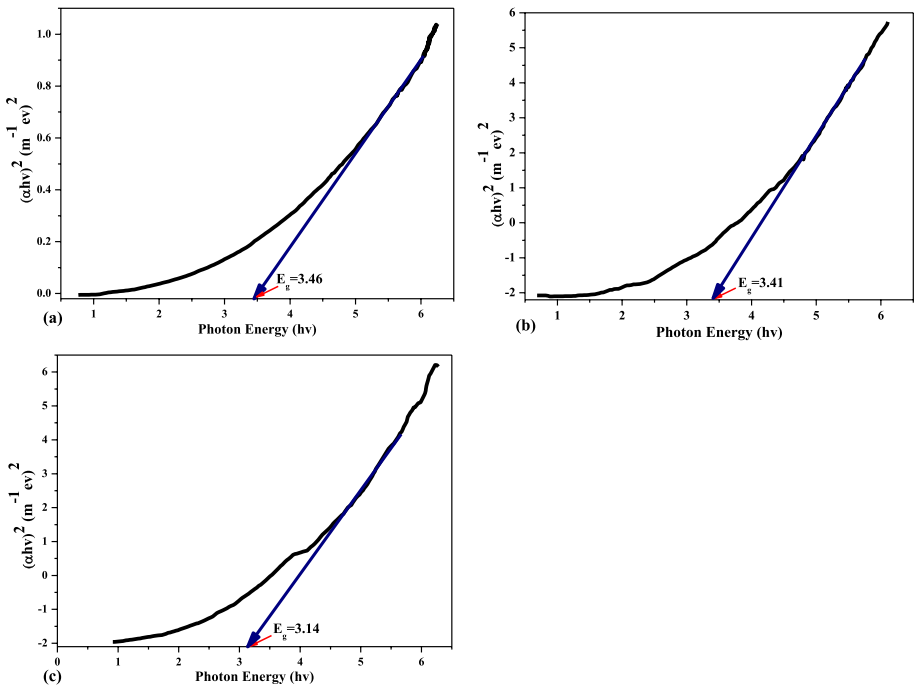


Fig. 6 Tauc plot of zinc oxide thin films deposited at substrate temperatures of **a** RT, **b** 300 °C and **c** 500 °C

where, R_0 is coefficient of linear reflection, I_0 is intensity of incident radiation, k_2 is nonlinear extinction, and n_2 is coefficients of nonlinear refraction.

$$G_m(z) = g(z) - i \frac{d}{d_m}, \text{ where } g(z) = \frac{d}{d_0}x \text{ and } d_m = \frac{k\omega_{m0}^2}{2}$$

$$\omega_{m0}^2 = \frac{\omega^2(z)}{2m+1}, \text{ where } \omega^2(z) = \omega_0^2(1+x^2) \text{ and } x = \frac{z}{z_0} \tag{7}$$

$$z_0 = \frac{k\omega_0^2}{2}, \text{ where } k = \frac{2\pi}{\lambda}$$

Here, ω_0 is beam radius at the waist, z_0 is diffraction length of the beam, d is distance from sample to the far-band orifice, k is the wave number, and z is the position of specimen. Without considering the impact of thermal processes, the amplitude reflection coefficient, $R_1(\theta)$ is:

$$R_1(\theta) = \frac{2n_0^3 \cos\theta - 4n_0 \cos\theta \sin^2\theta}{n_0^4 \cos^2\theta - n_0^2 + \sin^2\theta} [n_0^2 - \sin^2\theta]^{-1/2} \tag{8}$$

where θ is angle of incidence radiation & n_0 is linear refractive index.

Substituting parameters from Eqs. (8) and (7) in to Eq. (6), the expression for normalized reflection $R(z, \theta)$ is:

$$R(z, \theta) = 1 - \frac{\left(\frac{4R_1(\theta)}{R_0}\right) I_0 k_2 x}{(x^2 + 9)(x^2 + 1)} + \frac{\left(\frac{2R_1(\theta)}{R_0}\right) I_0 n_2 (x^2 + 3)}{(x^2 + 9)(x^2 + 1)} + \frac{\left(\frac{R_1(\theta)}{R_0}\right)^2 I_0^2 (n_2^2 + k_2^2)}{(x^2 + 9)(x^2 + 1)} \tag{9}$$

The 1st equation on the right is responsible for nonlinear absorption, the 2nd equation for nonlinear refraction, and the 3rd equation is for their combined impact.

Real part of third order nonlinear susceptibility was analysed using (Sheik-Bahae et al. 1990):

$$\text{Re}\chi^3 = \frac{n_0}{3\pi} n_2 \tag{10}$$

Refractive nonlinearities are measured without aperture in reflective z-scan, by eliminating the impact of phase changes due to non-linear absorption. In RZ-Scan, sample along with mirror is moved along focus plane and the intensity is maximum when sample is at focal plane and non-linear effect is appears. A reflecting Z-scan technique was employed to determine nonlinear refraction of non-transparent samples and its normalized reflectance is fitted to experimental data by using Eq. (9) above.

Figure 7 shows Normalized reflectance, $R(z)$ as a function of sample position without aperture for different deposition temperatures of (a) RT , (b) 300°C and (c) 500°C at wavelength of 532nm . The variation of $R(z)$ of samples for all temperatures shows the same shape of bell, that its top is directed upward. When the sample is at focal plane ($z = 0$), the reflection is symmetric and the intensity becomes maximum. This shows that, ZnO thin film samples exhibits positive refractive nonlinearities, which shows self-focusing ($n_2 > 0$) properties in the samples. As it can be concluded from the figure, the tops of the bell-shapes are higher for the samples deposited at high temperature (500°C).

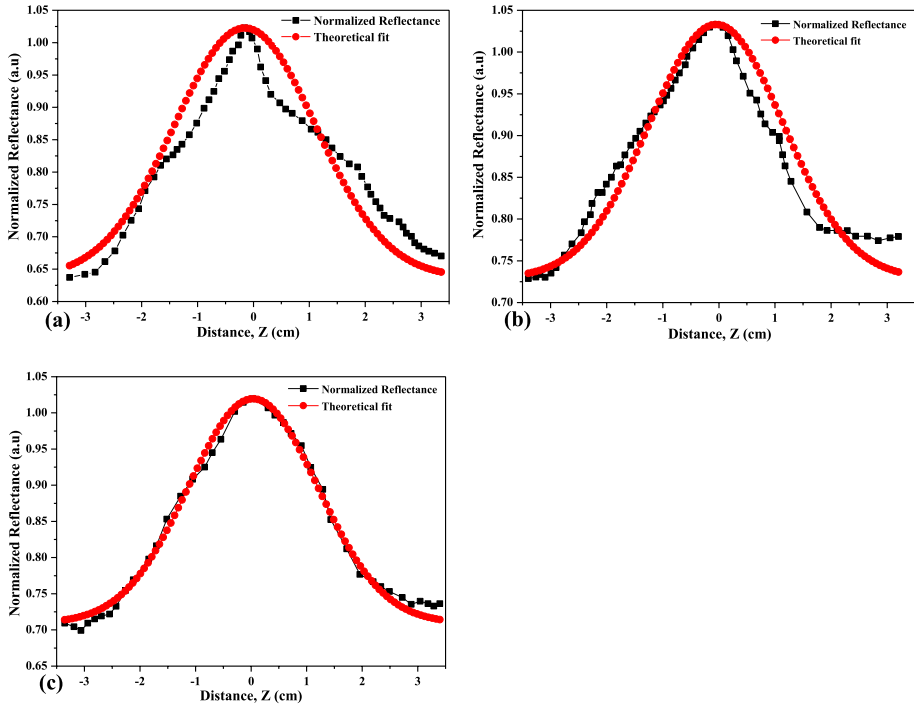


Fig. 7 Normalized reflectance as a function of sample positioned for open aperture z-scan of samples for various temperatures of **a** RT, **b** 300 °C and **c** 500 °C

The numerical fitting to experimental data of $R(z)$ were carried out by using Eq. (9) as it depicted in Fig. 7 and the valley peak curve is absent because of the 3^{rd} term in Eq. (9). By using $R(z)$ relations and fitting it to experimental data, nonlinear refractive index n_2 are calculated for all samples. Real part of third order nonlinear susceptibility, $Re\chi^3$ was determined by using Eq. (10). Nonlinear refractive index, n_2 & real part of third order nonlinear susceptibility, $Re\chi^3$ obtained in this work are listed in Table 2. Results shown in Table 2 indicates, both n_2 and $Re\chi^3$ increases as deposition temperatures of the zinc oxide samples increases (Henari and Dakhel 2010).

Table 2 Nonlinear optical parameters of zinc oxide thin films deposited at temperatures of RT, 300 °C & 500 °C, labelled S1, S2, S3 respectively

ZnO Thin films	$n_2 \left(\frac{cm^2}{w} \right)$	$Re\chi^3 \left(\frac{cm^2}{w} \right)$
S1	1.5×10^{-9}	3.18×10^{-10}
S2	2.9×10^{-9}	6.15×10^{-10}
S3	25.3×10^{-9}	5.37×10^{-10}

4 Conclusions

The various experimental carried out by different research groups proves that the ZnO thin film structures are an important nonlinear material that exhibits remarkable non-linearity under intense laser beams. In present studies Zinc oxide thin films was deposited by sol–gel techniques at various substrate temperatures of room temperature (RT), 300 °C and 500 °C. Structural characteristics of zinc oxide thin film samples at various substrate temperatures have been investigated by XRD patterns in the range of angle $10^\circ - 80^\circ$ using CuK_α (1.541Å) radiation. The occurrence of the wurtzite-type ZnO hexagonal phase and film growth along *c* axis were observed from XRD analysis. Surface morphology of Zinc oxide thin film samples are analysed using FE-SEM and branching like urchin morphology is observed and the size of rods and crystallites of thin films increases, when temperature is varied. Fourier transform infrared spectroscopic (FTIR) studies of zinc oxide thin film is performed using Nicolet Magana IR750 FTIR spectrometer in the wavelength range of 400cm^{-1} – 1500cm^{-1} . It is shown that, the band observed in this wave number range corresponds to vibrational stretching mode, water molecules found in zinc oxide thin film and symmetric C = O bond vibration and substrate temperature variations. Nonlinear optical properties of zinc oxide thin films were studied using reflective z-scan methods and its normalized reflectance is fitted to experimental data to calculate nonlinear reflective index, n_2 and $\text{Re}\chi^3$.

Acknowledgements We would like to thanks GJUS&T and WKU to give me chance to do this work.

Author contributions Getu Endale: Conceptualization, Methodology, Investigation, Writing, review & editing. Poonam: experimental analysis, Visualization, review & editing. Devendra Mohan: Supervision, Writing, review and editing.

Funding The authors have no any funding agencies.

Data availability The datasets generated during the current study are available from the corresponding author on request.

Declarations

Competing interests The authors declare no competing interests.

References

- Bacaksiz, E., Parlak, M., Tomakin, M., Ozelik, A., Karakiz, M., Altunbas, M.: The effect of zinc nitrate, zinc acetate and zinc chloride precursors on investigation of structural and optical properties of ZnO thin films. *J. Alloy. Compd.* **466**, 447–450 (2008)
- Banerjee, A.N., Gosh, C.K., Chattopadhyaya, K.K., Minoura, H., Sarkar, A.K., Akiba, A., Kamiya, A., Endo, T.: Low-temperature deposition of ZnO thin films on PET and glass substrates by DC-sputtering technique. *Thin Solid Films* **496**(1), 112–116 (2006). <https://doi.org/10.1016/j.tsf.2005.08.258>
- Bäuerle, D.W.: *Laser Processing and Chemistry*. Springer (2013)
- Boyd, I.W.: *Laser Processing of Thin Films and Microstructures: Oxidation, Deposition and Etching of Insulators* (Vol. 3). Springer.
- Chari, M., Matoussi, A.: Electrical conduction and dielectric studies of ZnO pellets. *Phys. B Condens. Matter* **407**, 3441–3447 (2012)

- Chen, X., An, C., Liu, J., Wang, X., Qian, Y.: Fabrication and characterization of hexagonal wire like ZnO. *J. Cryst. Growth* **253**, 357–360 (2003)
- Constantinescu, C., Rotaru, A., Nedelcea, A., Dinescu, M.: Thermal behavior and matrix-assisted pulsed laser evaporation deposition of functional polymeric materials thin films with potential use in optoelectronics. *Mater. Sci. Semicond. Process.* **30**, 242–249 (2015)
- Dikovska, A.O., Atanasov, P.A., Vasilev, C., Dimitrov, I.G., Stoyanov, T.R.: Thin ZnO Films Produced By Pulsed Laser Deposition. *J. Optoelectron Adv M* **7**, 1329–1334 (2005)
- Fan, X.M., Lian, J.S., Guo, Z.X., Lu, H.J.: ZnO thin film formation on Si(111) by laser ablation of Zn target in oxygen atmosphere. *J. Cryst. Growth* **279**, 447–453 (2005)
- Growbaska, J., Nanda, K.K., McGlynn, E., Mosnier, J.P., Henry, M.O.: Studying the growth condition, the alignment and structure of ZnO nanorods. *Surf. Coat. Technol.* **200**, 1093–1096 (2005)
- Henari, F.Z., Dakhel, A.A.: Investigation of nonlinear optical properties of gold nanograins embedded in indium oxide films by reflection Z-scan using continuous laser. *J. Appl. Phys.* **108**(12), 123109–1231095 (2010). <https://doi.org/10.1063/1.3524281>
- Irimpan, L., Deepthy, A., Krishnan, B., Nampoori, V.P., Radhakrishnan, P.: Nonlinear optical characteristics of self-assembled films of ZnO". *Appl. Phys. B* **556**(90), 547–556 (2008). <https://doi.org/10.1007/s00340-007-2886-1>
- Kepecio, A., Yi, S., Gündo, Y., Küçükçelebi, H., Kılıç, H.Ş.: ScienceDirect nonlinear optical properties of zinc oxide thin films produced by pulsed laser deposition. *Mater. Today Proc.* **18**, 1819–1825 (2019). <https://doi.org/10.1016/j.matpr.2019.06.669>
- Kim, H.W., Kim, N.H., Lee, C., Ryu, J.H., Lee, N.E.: Deposition-Temperature Dependence of ZnO/Si Grown by Pulsed Laser Deposition. *J. Korean Phys. Soc.* **44**(14), S685–S688 (2004)
- Komaraiah, D., Radha, E., Vijayakumar, Y., Sivakumar, J., Reddy, M.R., Sayanna, R.: Optical, Structural and Morphological Properties of Photocatalytic ZnO Thin Films Deposited by Pray Pyrolysis Technique, *Modern research in catalysis.* **5**(4), 130–146 (2016)
- Laurenti, M., Cauda, V.: Porous zinc oxide thin films: synthesis approaches and applications. *Coatings* **8**, 67–91 (2018). <https://doi.org/10.3390/coatings8020067>
- Liu, W., Wang, B., Fan, J., Ge, Y.: A quantum system control method based on enhanced reinforcement learning. *Soft. Comput.* **26**(14), 6567–6575 (2022)
- Li, Q.H., Liang, Y.X., Wan, Q., Wang, T.H.: Oxygen sensing characteristics of individual ZnO nanowire transistors. *Appl. Phys. Lett.* **85**, 6389–6391 (2004)
- Li, G., Wang, W., Yang, W., Wang, H.: Epitaxial growth of group III-nitride films by pulsed laser deposition and their use in the development of LED devices. *Surf. Sci. Rep.* **70**(3), 380–423 (2015)
- Martinelli, M., Gomes, L., Horowicz, R.J.: Measurement of refractive nonlinearities in GaAs above band-gap energy. *Appl. Opt.* **39**(33), 6193 (2000). <https://doi.org/10.1364/ao.39.006193>
- Ma, T.Y., Kim, S.H., Moon, S.H.Y., Park, G.C., Kim, Y.J., Kim, K.W.: Substrate Temperature Dependence of ZnO Films Prepared by Ultrasonic Spray Pyrolysis. *Jpn. J. Appl. Phys.* **35**(12), 6208–6211 (1996)
- Morosanu, C.E.: *Thin Films by Chemical Vapour Deposition.* Elsevier, Amsterdam (1990). (**Chapter 2**)
- Mosca, D.C.R., Zanichelli, M., Villani, M., Zappettini, A.: Aldehyde detection by ZnO tetrapod-based gas sensors. *J. Mater. Chem.* **21**, 15532–15536 (2011)
- Oruç, F.B., Cimen, F., Rizk, A., Ghaffari, M., Nayfeh, A., Okay, A.K.: Thin-film ZnO charge-trapping memory cell grown in a single ALD step. *IEEE Electron Device Lett.* **33**(12), 1714–1716 (2012)
- Rajalekshmi, E.S., Raj, A.M.E.: Effect of substrate temperature on structural and morphological studies by spray pyrolysed ZnO thin films. *Solid State Commun.* **338**, 1–4 (2021). <https://doi.org/10.1016/j.ssc.2021.114479>
- Sadananda Kumar, N., Banger, K.V., Shivakumar, G.K.: Effect of annealing on the properties of zinc oxide nanofiber thin films grown by spray pyrolysis technique. *Appl. Nanosci.* **4**(2), 209–216 (2013). <https://doi.org/10.1007/s13204-012-0190-9>
- Sagadevan, S., Vennila, S., Anita Lett, J., Marlinda, A.R., Aliya Binti Hamizi, N., Rafie Johan, M.: Tailoring the structural, morphology, optical and dielectric characteristics of ZnO nanoparticles using Starch as a capping agent. *Results Phys.* **15**, 1–6, (2019). <https://doi.org/10.1016/j.rinp.2019.102543>
- Sandeep, K.M., Bhat, S., Dharmaprakash, S.M.: Structural, optical, and LED characteristics of ZnO and Al doped ZnO thin films. *J. Phys. Chem. Solids* **104**, 36–44 (2017). <https://doi.org/10.1016/j.jpcs.2017.01.003>
- Schroder, D.K.: *Semiconductor Material and Device Characterization.* Wiley, New York (1990)
- Sheik-Bahae, M., Said, A.A., Wei, T.-H., Hagan, D.J., Van Stryland, E.W.: Sensitive measurement of optical nonlinearities using a single beam. *IEEE J. Quantum Electron.* **26**(4), 760–769 (1990). <https://doi.org/10.1109/3.53394>

- Song, D., Widenborg, P., Chin, W., Aberle, A.: Investigation of lateral parameter variations of Al-doped zinc oxide films prepared on glass substrates by rf magnetron sputtering. *Sol. Energy Mater. Sol. Cells* **73**, 269 (2002)
- Srinatha, N., Raghu, P., Mahesh, H.M., Angadi, B.: Spin-coated Al-doped ZnO thin films for optical applications: Structural, micro-structural, optical and luminescence studies. *J. Alloy. Compd.* **722**, 888–895 (2017). <https://doi.org/10.1016/j.jallcom.2017.06.182>
- Srinivasulu, T., Saritha, K., Reddy, K.T.R.: Synthesis and characterization of Fe-doped ZnO thin films deposited by chemical spray pyrolysis. *Mod. Electron. Mater.* **3**(2), 76–85 (2017). <https://doi.org/10.1016/j.moem.2017.07.001>
- Sucnea, M., Christoulakis, S., Katsarakis, N., Kitsopoulos, T., Kiriakidis, G.: Comparative study of ZnO and Al-doped ZnO transparent thin films grown by DC magnetron sputtering. *Thin Solid Films* **515**, 6562–6566 (2007)
- Talam, S., Karumuri, S.R., Gunnam, N.: Synthesis, characterization, and spectroscopic properties of ZnO nanoparticles. *ISRN Nanotechnol.* **2012**, 1–6 (2012). <https://doi.org/10.5402/2012/372505>
- Tite, T., Donnet, C., Loir, A.S., Reynaud, S., Michalon, J.Y., Vocanson, F., Garrelie, F.: Graphene-based textured surface by pulsed laser deposition as a robust platform for surface enhanced Raman scattering applications. *Appl. Phys. Lett.* **104**(4), 041912–4 (2014)
- Vanalakar, S.A., Agawane, G.L., Shin, S.W., Suryawanshi, M.P., Gurav, K.V., Jeon, K.S., Patil, P.S., Jeong, C.W., Kim, J.Y., Kim, J.H.: A review on pulsed laser deposited CZTS thin films for solar cell applications. *J. Alloy. Compd.* **619**, 109–121 (2015)
- Willey, R.R.: *Field Guide to Optical Thin Films*. SPIE Press, Bellingham (1936)
- Yakubu, A., Abbas, Z., Hashim, M., Fahad, A.: Effect of sintering temperature on Co_{0.5}Zn_{0.5}Fe₂O₄ nanoparticles evolution and particle size distribution. *Adv. Nanoparticles* **4**, 37–44 (2015). <https://doi.org/10.4236/anp.2015.42005>
- Yang, Z., Ye, Z., Xu, Z., Zhao, B.: Effect of the morphology on the optical properties of ZnO nanostructures. *Physica e: Low-Dimens Syst Nanostruct* **42**(2), 116–119 (2009). <https://doi.org/10.1016/j.physe.2009.09.010>
- Zhang, K., Du, X., Katz, M.B., Li, B., Kim, S.J., Song, K., Graham, G.W., Pan, X.: Creating high quality Ca: TiO₂-B (CaTi₅O₁₁) and TiO₂-B epitaxial thin films by pulsed laser deposition. *Chem. Commun.* **51**(41), 8584–8587 (2015)
- Zhu, H., Fu, Y., Meng, F., Wu, X., Gong, Z., Ding, Q., Gustafsson, M.V., Trinh, M.T., Jin, S., Zhu, X.Y.: Lead halide perovskite nanowire lasers with low lasing thresholds and high quality factors. *Nat. Mater.* **14**(6), 636–642 (2015)
- Zidan, M.: A novel quantum computing model based on entanglement degree. *Mod. Phys. Lett. B* **34**(35), 2050401–2050411 (2020)
- Zidan, M., Abdel-Aty, A.H., Khalil, A., Abdel-Aty, M., Eleuch, H.: A novel efficient quantum random access memory. *IEEE Access* **9**, 151775–151780 (2021)
- Zidan, M., Eldin, M.G., Shams, M.Y., Tolan, M., Abd-Elhamed, A., Abdel-Aty, M.: A quantum algorithm for evaluating the hamming distance. *Comput. Mater. Continua* **71**(1), 1065–1078 (2022)
- Zidan, M., Hegazy, S.F., Abdel-Aty, M., Obayya, S.S.: Rapid solution of logical equivalence problems by quantum computation algorithm. *Appl. Soft Comput.* **132**, 109844–55 (2023)

Publisher's Note Springer Nature remains neutral with regard to jurisdictional claims in published maps and institutional affiliations.

Springer Nature or its licensor (e.g. a society or other partner) holds exclusive rights to this article under a publishing agreement with the author(s) or other rightsholder(s); author self-archiving of the accepted manuscript version of this article is solely governed by the terms of such publishing agreement and applicable law.